CHAPTER 6

Laser Microsurgery in *Caenorhabditis elegans*

Christopher Fang-Yen[*], Christopher V. Gabel[†], Aravinthan D. T. Samuel[‡], Cornelia I. Bargmann[§] and Leon Avery[¶]

[*]Department of Bioengineering, University of Pennsylvania, Philadelphia, PA, USA

[†]Department of Physiology and Biophysics, Boston University School of Medicine, Boston, MA, USA

[‡]Department of Physics and Center for Brain Science, Harvard University, Cambridge, MA, USA

[§]Howard Hughes Medical Institute and The Rockefeller University, New York, NY, USA

[¶]University of Texas Southwestern Medical Center, Dallas, TX, USA

METHODS IN CELL BIOLOGY, VOL 107

0091-679X/10 $35.00
DOI 10.1016/B978-0-12-394620-1.00006-0

Abstract

Laser killing of cell nuclei has long been a powerful means of examining the roles of individual cells in *C. elegans*. Advances in genetics, laser technology, and imaging have further expanded the capabilities and usefulness of laser surgery. Here, we review the implementation and application of currently used methods for target edoptical disruption in *C. elegans*.

I. Overview

One way to study *in vivo* cell function is to eliminate the cell and observe subsequent developmental or behavioral abnormalities in the animal. In *Caenorhabditis elegans*, this can be done by killing individual cells or groups of cells with a laser microbeam. Laser killing has been used to determine the functions of many cell types, including neurons involved in locomotion, feeding, mechanosensation, and chemosensation (Avery and Horvitz, 1989; Bargmann *et al*., 1993; Bargmann and Horvitz, 1991a; Chalfie *et al*., 1985; Gabel *et al*., 2007; Gray *et al*., 2005; Li *et al*., 2006; Tsalik and Hobert, 2003; Ward *et al*., 2008). These studies have been practical because only a few cell types are required for nematode viability (Avery and Horvitz, 1987; Bargmann and Horvitz, 1991b; J. Sulston, personal communication).

Laser ablation can also be used to study interactions among cells during development. Signaling and inductive interactions between cells can be examined by removing one cell and observing the development of the remaining cells. For example, killing the distal tip cells of the somatic gonad causes premature differentiation of the germ line, showing a role for the somatic gonad in maintenance of the germ line in an undifferentiated state (Kimble and White, 1981). In some cases, laser killing has also revealed that multiple cells can be competent to adopt certain fates, and another cell can substitute itself in the absence of the normal precursor (Sulston and White, 1980). For example, if the precursor to the anchor cell of the somatic gonad is killed, another cell becomes the anchor cell, but the uterine cells usually generated by the second cell are absent (Kimble, 1981). Postembryonic cell interactions in the developing gonad, the hermaphrodite vulva, and the male tail have been particularly well characterized using laser killing (Chamberlin and Sternberg, 1993; Kimble, 1981; Kimble and White, 1981; Sulston and White, 1980). Other cells have been found to regulate specific aspects of each other's development, such as cell migrations and axon outgrowth (Garriga *et al*., 1993; Li and Chalfie, 1990; Thomas *et al*., 1990; Walthall and Chalfie, 1988).

The developmental potential of cells in the early embryo has also been explored by laser killing (Priess and Thomson, 1987; Schnabel, 1994; Sulston *et al*., 1983). These experiments are particularly useful because the classic embryological manipulations of transplantation and microdissection are so far only possible for the first few blastomeres of the *C. elegans* embryo.

Laser killing can assist in the interpretation of mutant phenotypes. If a cell interaction or cell function has been defined by killing a cell, genes that affect that cell's signaling capacity or viability may be identified by isolating mutants with phenotypes similar to that caused by cell killing (Austin and Kimble, 1987; Bargmann *et al*., 1993; Ferguson and Horvitz, 1985; McIntire *et al*., 1993). In addition, killing cells in mutant animals can provide information about which cells mediate the defects associated with a mutation (Bargmann and Horvitz, 1991b; Li *et al*., 2006; Mello *et al*., 1992; Ward *et al*., 2008; Waring and Kenyon, 1990).

Laser ablation can also be used to probe cell function in nematode species that are not accessible to genetic analysis. Laser killing of vulval cell precursors has been used to elucidate cell interactions in *Mesorhabditis* and *Teratorhabditis* nematodes (Sommer and Sternberg, 1994). Laser killing of pharyngeal neurons has been used to compare their roles in pharyngeal behaviors in nematodes from the *Diplogasteridae*, *Cephalobidae*, and *Panagrolaimidae* families (Chiang *et al*., 2006), and laser killing has been used to map sensory behaviors in multiple *Caenorhabditis* species, as well as *Panagrellus, Pristionchus,* and *Strongyloides* nematodes (Forbes *et al*., 2004; Srinivasan *et al*., 2008).

Individual *C. elegans* cells can be killed by a laser microbeam focused through the objective of a microscope. The first apparatus used for this purpose was developed by John White (Sulston and White, 1980). Subsequent technical refinements made this technique easier and more reproducible (J. G. White, personal communication and Avery and Horvitz, 1987). The laser beam is focused in three dimensions on a single spot in the field of view of a microscope. A cell of interest is aligned with the laser beam. Damage to the cell and adjacent structures can be observed through the microscope during and after the operation. Any cell can be killed with a laser microbeam in this manner, but this chapter is biased toward neurons because of the expertise of the authors.

Laser microbeams can also be used to sever individual *C. elegans* nerve fibers (Gabel, 2008). Using this technique, Yanik *et al.* showed that motor neuron axons regrow after being cut (Yanik *et al*., 2004), pioneering *C. elegans* as a model for nerve regeneration. Subsequent studies have elucidated cellular and molecular mechanisms mediating axonal regrowth after damage (Gabel *et al*., 2008; Ghosh-Roy *et al*., 2010; Hammarlund *et al*., 2009; Wu *et al*., 2007; Yan *et al*., 2009).

Laser severing of nerve processes can be useful for understanding roles of specific neural processes in generating or transmitting sensory or motor information. In some cases, laser cutting nerve fibers and whole-cell ablations lead to similar deficits, indicating that the nerve fiber is required for the function being assayed. Cutting GABAergic motor neuron axons led to deficits in reverse locomotion similar to those in worms for which GABA motor neurons had been laser killed (McIntire *et al*., 1993; Yanik *et al*., 2004). Severing the sensory dendrite of AFD thermosensory neurons abolished their contribution to temperature-sensing behavior (Chung *et al*., 2006). Imaging of calcium dynamics in AFD neurons with severed

dendrites showed that both temperature detection and the storage of a preferred temperature "memory" occurs at its sensory endings (Clark *et al.*, 2006).

In other cases, axotomy and cell killing have different effects. Laser ablation of the HSN neurons greatly reduces the worm's egg laying frequency (Desai and Horvitz, 1989; Trent *et al.*, 1988). However, laser-cutting of HSN axons between the nerve ring and vulva does not appreciably affect egg-laying behavior, and laser-cutting of HSN axons between the cell body and vulva does not affect HSN calcium activity, suggesting that HSN activity does not require synaptic input (Zhang *et al.*, 2008).

II. Identifying Cells in *C. elegans*

Unambiguous identification of cells is essential for any experiment involving laser ablation. Rigorous identification of a cell type can be accomplished by following cell lineages through embryonic or postembryonic divisions (Kimble and Hirsh, 1979; Sulston and Horvitz, 1977; Sulston *et al.*, 1983; Sulston and White, 1980). This approach is practical if a cell can be killed soon after its birth; it is the only method that works well for many blast cells in the embryo. Following cell divisions can be time consuming, but, fortunately, most cells in *C. elegans* are found in reproducible positions. Therefore, a combination of morphological characters and position can usually be used to identify the cells in wild-type animals without following cell lineages.

When viewed using Nomarski optics, the nuclei of different cell types have characteristic appearances (Fig. 1). Hypodermal nuclei and gut nuclei have a "fried egg" appearance; they are round and smooth in texture with large, prominent nucleoli. Neuronal nuclei are smaller and round, lack prominent nucleoli, and have a punctate nucleoplasm ("pepperoni" appearance). Muscle nuclei are oblong, are intermediate in size between neuronal and hypodermal nuclei, and have a punctate nucleoplasm and a small nucleolus. The optimal time for finding a cell depends on the particular cell type. Most cells are most easily seen using Nomarski microscopy in very young larvae. As the animals grow, visualization of cells in deep focal planes becomes more difficult. Many neurons can be identified at the beginning of the first larval stage (L1) (Fig. 2). In the pharynx, nuclei may be easier to see in the L2 stage. Cells in the pharynx can be identified by using the diagrams in Fig. 3. The pharynx and nerve ring do not change much during postembryonic development.

Once postembryonic divisions begin (about 5 h after hatching), it might be necessary to stage the animals carefully or follow cell lineages to identify cells unambiguously in the body and tail. Embryonic and postembryonic blast cells are described in detail in (Sulston *et al.*, 1983) and (Sulston and Horvitz, 1977).

A few stages can be learned as starting points for following lineages, including the 28-cell stage in the embryo (Fig. 4), the B$\alpha/\beta/\gamma/\delta$ stage in the male tail, and the 12-cell stage at the hermaphrodite vulva (Sulston and Horvitz, 1977). Some cells cannot be reliably identified on the basis of position because of natural variability in their location. The most difficult areas are (1) the posterior lateral ganglia in the head

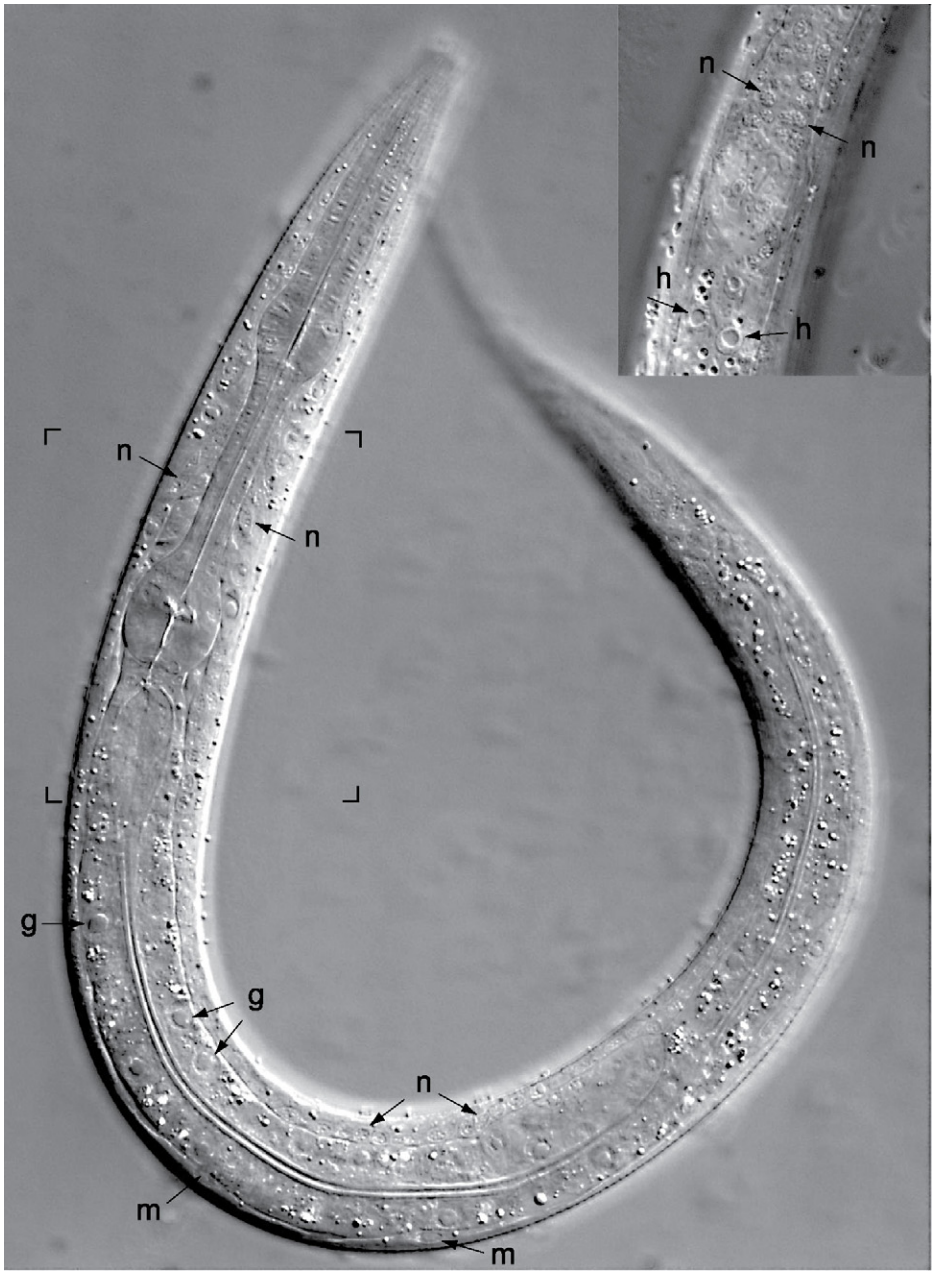

Fig. 1 Appearance of different cell types. L1 animal viewed by Nomarski optics. Inset: View of region near terminal bulb (as marked) with focal plane near surface of worm. h, hypodermal nucleus; n, neuronal nucleus; g, gut nucleus; m, muscle nucleus.

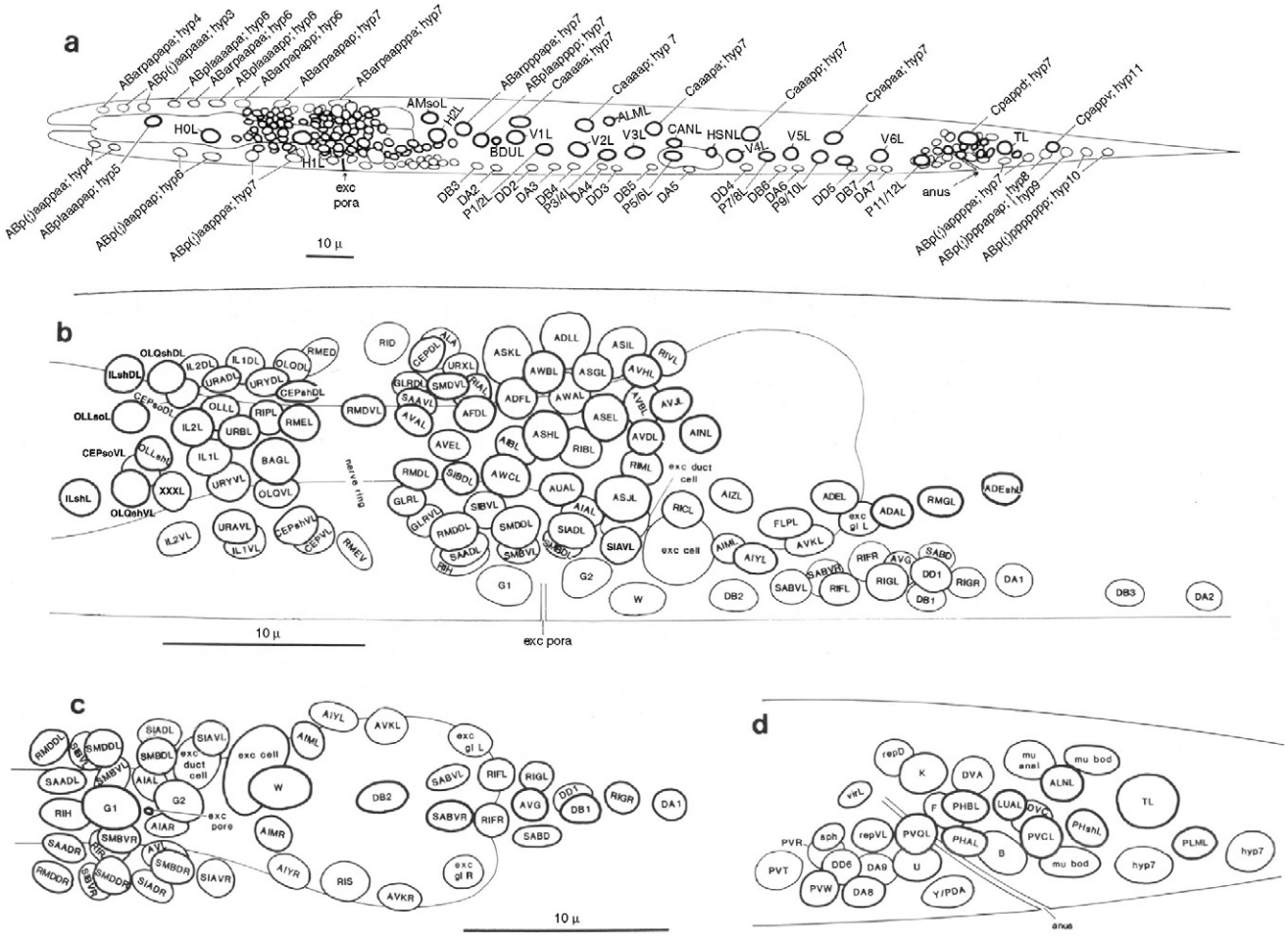

Fig. 2 Positions of nuclei in L1 larvae. (a) Positions of nuclei in L1 larvae (left lateral view). (b) Neuronal nuclei in the head (left lateral view). (c) Neuronal nuclei in the head (ventral view). (d) Neuronal nuclei in the tail (left lateral view). Anterior is the left. In a, b, and d, only the left lateral nuclei and the medial nuclei are shown. Most right lateral nuclei occupy positions similar to those of their homologs on the left side; the exceptions are found most on the ventral side (see c). The thickness of the nuclear outline is inversely related to the depth of the nucleus within the worm (e.g. in b, lateral nuclei have thick outlines and medial nuclei have thin outlines). Reprinted, with modifications, from (Sulston *et al*., 1983).

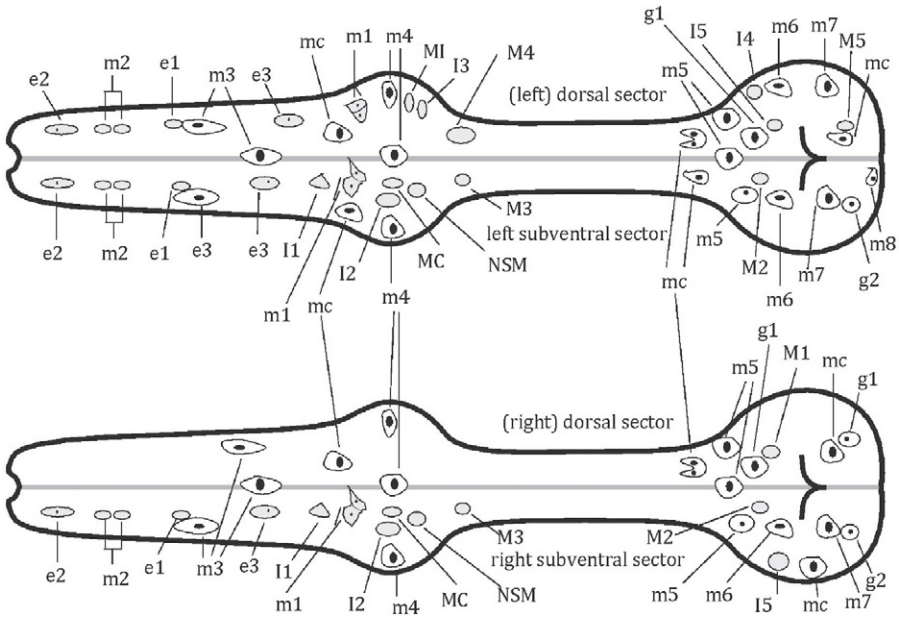

Fig. 3 Positions of nuclei in the pharynx. Modified from a drawing by Ron Ellis.

(AIN, RIC, AIZ, ADEso, and AVD), (2) the anterior socket and sheath cells in the head (AMSo, ILsh, ILso, and OLQso), (3) postembryonic neurons in the tail, and (4) postembryonic neurons in the ventral nerve cord.

It is easiest to learn the position of particular cells in animals in which one or more cell types are fluorescently labeled. Worms that express GFP or another fluorescent protein in the cells to be ablated can be used to identify cells. Alternatively, lipophilic fluorescent dyes such as fluorescein isothiocyanate (FITC) (Hedgecock *et al*., 1985), DiI, and DiO (Collet *et al*., 1998) can be used to stain the amphid neurons (ASI, ADL, ASK, AWB, ASH, and ASJ) and the phasmid neurons (PHA and PHB). A dye-filling protocol for labeling the IL2 neurons has also been developed (Burket *et al*., 2006). Simultaneous observation of Nomarski images and fluorescent images of these cells can be used to learn their positions. Once these cells are familiar, it can be relatively simple to identify adjacent cells. Similarly, fixed animals can be doubly stained with an antibody and 4′,6-diamidino-2-phenylindole (DAPI, which strains all nuclei). Comparison of the fluorescent images can be used to learn the position of a cell for subsequent identification in live animals.

High-intensity optical illumination during fluorescence microscopy can cause photobleaching and cell damage, so both the intensity and duration of fluorescence illumination should be minimized during the laser operation procedure. The use of a sensitive camera will allow visualization of fluorescence at relatively low illumination intensity, and also provide for documentation of experimental procedures, if needed.

To perform laser cutting of nerve fibers, it is essential to have a fluorescent marker in the cell of interest, since nerve fibers are not visible under Nomarski microscopy.

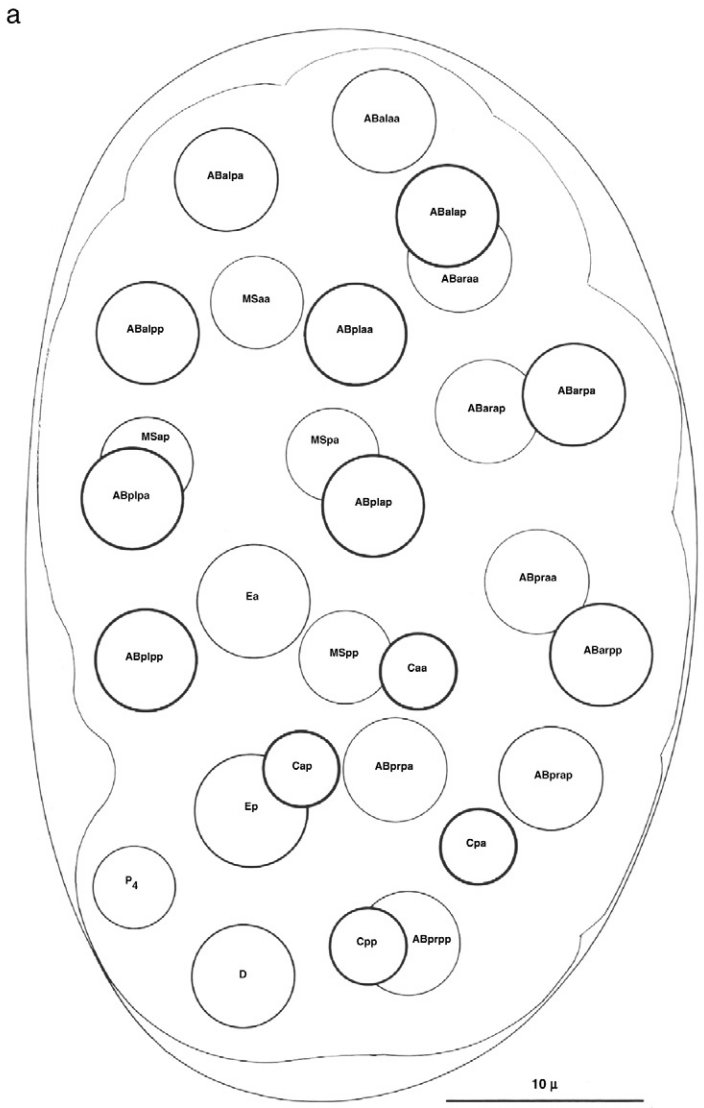

Fig. 4a Embryonic nuclei. (a) Twenty-eight-cell embryo 100 min, left dorsal aspect. (b) Embryo, 260 min, dorsal aspect, superficial nuclei. (c), Embryo, 270 min, ventral aspect, superficial nuclei. Anterior is at top. The thickness of the nuclear outline is inversely related to the depth of the nucleus within the worm. Nuclei undergoing cell death are darkened. Reprinted, with permission, from (Sulston et al., 1983). For detailed descriptions of embryonic and postembryonic cell divisions, see (Sulston and Horvitz, 1977), (Kimble and Hirsh, 1979), and (Sulston *et al*., 1983).

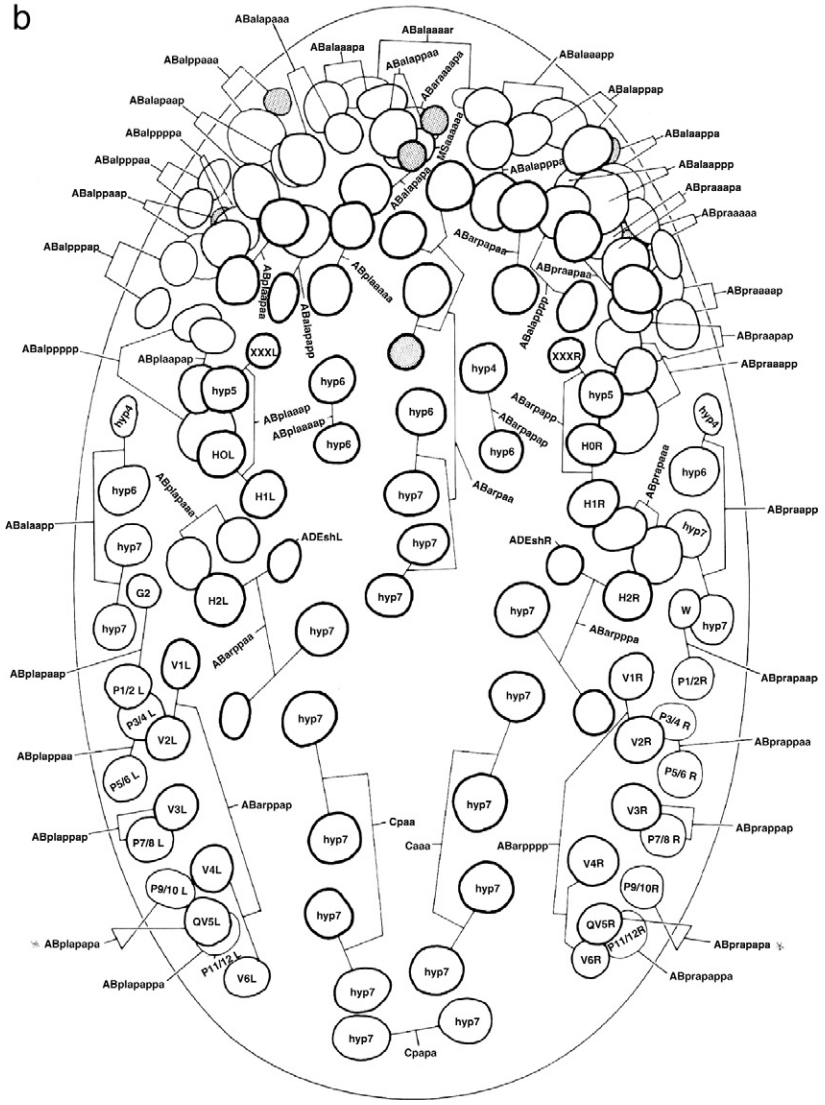

Fig. 4b (*Continued*)

The marker is usually GFP or another fluorescent protein. Laser surgery of sensory dendrites has also been performed after staining with lipophilic dyes (Chung *et al*., 2006). In our subsequent discussions we will refer to GFP, although any fluorescent marker can be used.

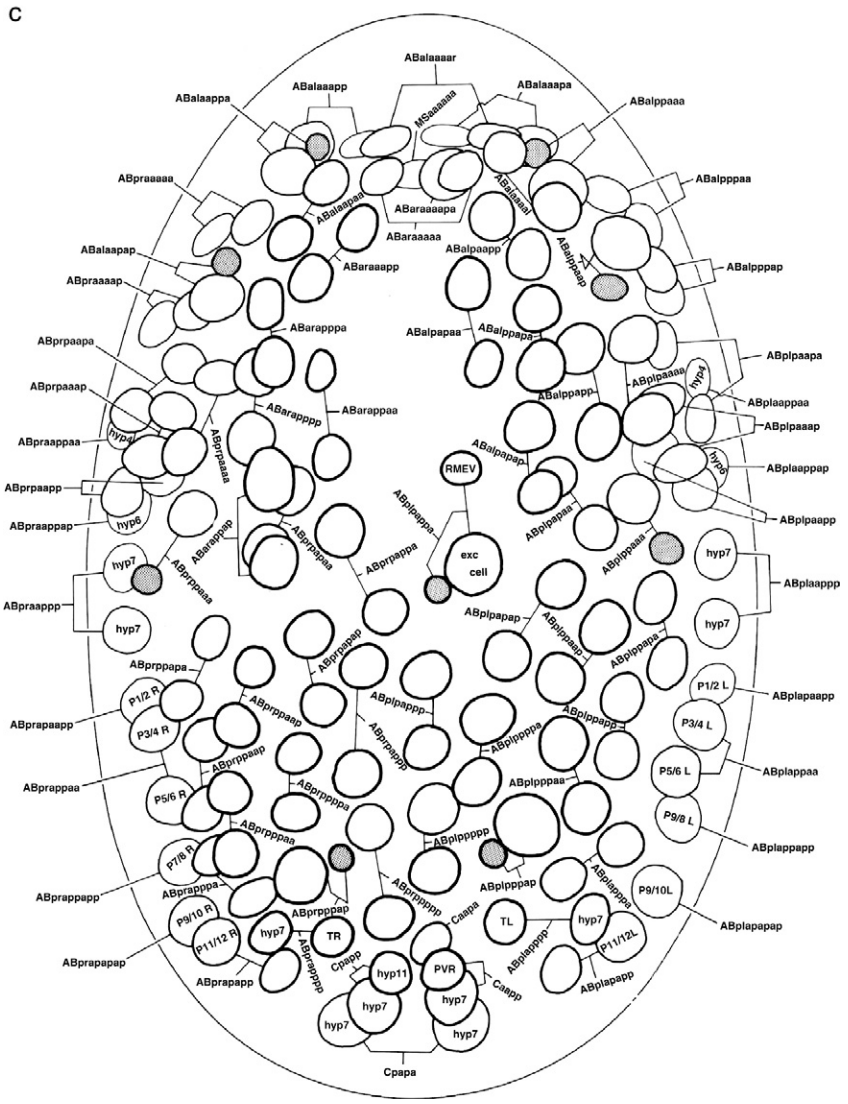

Fig. 4c (*Continued*)

III. Laser Ablation Theory and Apparatus

A. Tissue Damage by Nanosecond and Femtosecond Lasers

The physical mechanisms by which focused, pulsed laser beams cause tissue damage depend on the parameters of the laser used (Vogel *et al*., 2005; Vogel and Venugopalan, 2003). Pulsed laser systems are characterized by several parameters:

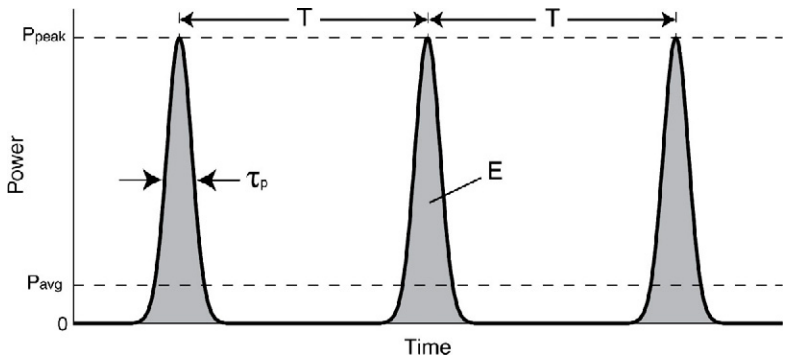

Fig. 5 Power as a function of time for a pulsed laser, showing peak power P_{peak}, average power P_{avg}, pulse width τ_p, pulse energy E, and repetition rate $1/T$. Pulse energy is the area under the curve for one pulse. (Note: for typical pulsed lasers, the ratio τ_p/T is much smaller than illustrated here.).

the center wavelength, the duration of a pulse, the peak power, the average power, repetition rate, and the energy per pulse (Fig. 5). Two types of lasers used for *C. elegans* microsurgery can be distinguished by their pulse durations:

(i) *Nanosecond lasers*: Nitrogen laser-pumped or diode laser-pumped dye laser are typically configured to produce violet/blue light with pulse durations of several nanoseconds and pulse energies up to several mega Joules. Pulse repetition rates typically range from 0 to 15 Hz.

(ii) *Femtosecond lasers*: Laser-pumped titanium-sapphire lasers are typically configured to produce near-infrared pulses with a center wavelength of approximately 800 nm, duration ~100–200 femtoseconds, pulse energies up to 50 nJ, and repetition rates of 80 MHz. Two methods can be used to reduce the repetition rate to a much smaller value (e.g., 1 kHz). In pulse picking, a fast optical modulator (usually electro-optic) positioned between the laser and the microscope allows only a small fraction of pulses to pass. In cavity dumping, also known as Q-switching, an optical switch (usually acousto-optic) located inside the laser cavity periodically allows the much more powerful laser beam circulating inside the laser resonator to escape. Cavity dumping thus generates a beam with lower repetition rate but higher laser pulse energy.

Nanosecond lasers were the first lasers used to kill *C. elegans* cells and they are most widely used for cell killing because of their relatively low cost and compact size. Femtosecond lasers, which are larger and much more expensive, are preferred for laser axotomy because of their ability to create more focused damage to the target and less damage to surrounding tissues (see below). Femtosecond lasers are also suitable for cell killing.

The damage caused by both nanosecond and femtosecond lasers is mediated by a process known as optical breakdown or laser-induced plasma formation (Vogel *et al*., 2005). The high electric field strength at the focus of a pulsed laser beam causes free

electrons in the material to be accelerated with sufficient energy to liberate additional electrons. The resulting avalanche process rapidly creates localized plasma capable of breaking chemical bonds and potentially vaporizing water and other tissue components. Local vaporization may generate a transient bubble that may cause additional thermal and mechanical disruption of the tissue.

The differences in damage between nanosecond and femtosecond ablation arise in part from the very different pulse energies required to achieve optical breakdown. The peak power per area at the focus of a pulsed laser scales with the pulse energy divided by the pulse duration. Therefore nanosecond pulses require much higher pulse energy compared with femtosecond pulses: pulse energies used for nanosecond ablation are typically tens of μJ, compared to tens of nJ for femtosecond ablation. The higher energy in nanosecond ablation generates more severe mechanical effects beyond the region of laser energy deposition (Vogel *et al*., 2005).

Femtosecond lasers have been used for laser surgery at both low (∼1 kHz) and high (∼80 MHz) repetition rates. An advantage of low repetition rates is that the deposited energy dissipates almost completely during the intervals between pulses (Shen *et al*., 2005). As a result, the laser beam may be focused onto a point in the sample indefinitely with minimal damage to surrounding tissues. A comparison of 80 MHz and 1 kHz ablation revealed differences in physical mechanisms, but concluded that both have superior spatial resolution compared to nanosecond ablation (Vogel *et al*., 2005). Surgery using the three types of laser irradiation (1 kHz femtosecond pulses, 80 MHz femtosecond pulses, and nanosecond pulses) vary in the size of a gap induced in a severed axon and in the extent of damage to surrounding tissues, but it appears that axon regeneration occurs at comparable rates and to comparable extents after axotomy using any of these techniques (Wu *et al*., 2007).

B. The Laser Apparatus

A laser surgery system consists of a laser, a microscope, and optics to direct the beam of the laser into the microscope objective. The microscope and laser are almost always purchased as off-the-shelf units. In many cases, customized optics that couple the laser and the microscope can also be purchased, so that relatively little optical alignment needs to be performed by the end user.

1. Components

Microscope

A high magnification compound microscope with Nomarski differential interference contrast optics and/or epifluoresence capabilities is necessary. The objective should have a numerical aperture of at least 1.25 in order to focus the laser beam to a sufficiently small spot. A low-power objective (e.g., 10×) can be useful for finding the worms on the slide.

The microscope must be capable of simultaneous imaging and laser exposure. For setups using Nomarski imaging, the laser beam may be introduced through the optical port normally used for epifluorescence illumination. A beam splitter is needed to reflect the laser light into the specimen while allowing light transmitted through the specimen to reach the eyepiece and/or camera for imaging. A barrier filter is also necessary to prevent reflected laser light from reaching the eyepiece. For the wavelengths typically used with nanosecond lasers, the beam splitter and barrier (or emission) filter from a fluorescein or GFP filter set work well. The excitation filter, which is between the light source and the beam splitter, should be removed.

To enable fluorescence imaging of target cells during the laser operation, a somewhat more complex system is necessary, since the epifluorescence port is now used. Microscope systems can be configured to allow simultaneous fluorescence and laser illumination. Some designs use a separate laser port within the fluorescence illumination path allowing simultaneous exposure of both light sources through a customized filter set. Other designs introduce a second laser-specific filter set behind the objective, leaving the fluorescence illumination pathway largely unchanged.

Laser

Nanosecond laser systems that attach directly to the microscope through the fluorescence illumination pathway and include all necessary coupling optics are now available. One such system is the Micropoint laser ablation system, a diode laser-pumped pulsed dye laser that can be configured for several types of microscopes and is sold by Photonic Instruments (Arlington Heights, IL). For most *C. elegans* researchers such a "turn-key" system will be the most convenient choice.

Two-photon imaging microscopes, which are often available in shared imaging facilities, usually contain femtosecond laser systems and are often suitable for laser cutting of nerve fibers. Two-photon and/or confocal imaging can be used to image the fluorescent nerve fiber to be severed. Next, the user can direct the microscope control software to perform a single-pass line scan over a short ($\sim$1–2 μm) path that traverses the fiber, at a laser power sufficiently high to sever the fiber. Two-photon and/or confocal imaging can be repeated (with laser power appropriate for normal imaging) to assess damage to the nerve fiber. Imaging the damaged area with Nomarski microscopy is also critical to assess nonspecific damage to nearby cells and tissues. Protocols for laser power and exposure time can be determined largely by trial and error. Start with the maximum power available and the shortest scan possible. If the laser does not cut the fiber, increase the exposure time. If the laser cuts the fiber, try a series of cuts with the laser power reduced by different amounts. The goal is to set a power and exposure time which reliably cut the axon while minimizing tissue damage.

Stand-alone femtosecond laser systems can be purchased from a number of companies including Coherent (Santa Clara, CA) and Newport Spectra Physics (Santa Clara, CA).

Lasers sufficiently powerful to perform surgery in *C. elegans* can cause skin and eye injuries to humans and should be taken seriously. In particular, setting up and aligning the laser can expose the user to dangerous stray beams. Laser safety glasses appropriate for the wavelength of the laser being used should be worn during alignment procedures and as necessary during routine use. For infrared lasers, an appropriate imaging card (e.g., Thorlabs VRC-4 or Newport F-IRC) is necessary to locate and observe the beam. Laser beam paths should generally be enclosed by opaque covers and kept well below eye-level of users. Be careful of specular reflections from mirrors, microscope slides, and other shiny objects. (Diffuse reflections, e.g., from a piece of paper, are not dangerous.) Safety guidelines appropriate for the specific laser and laboratory should always be followed.

Optics

Purchase and alignment of coupling optics are required only if they are not included as part of a turn-key system. Coupling optics do two things. First, they shape the beam so that it enters the specimen from the full available range of angles and comes to sharp focus at the image plane. Second, they allow beam location and angle to be adjusted. Lenses and mirrors can be mounted in optical positioners that allow fine, stable, and continuous adjustment. Coupling optics, mounts, and positioners may be purchased from companies such as Thorlabs (Newton, NJ), Newport (Irvine, CA), or New Focus (San Jose, CA).

Figure 6 shows the optical configurations used to shape the beam and focus it onto the specimen. Our discussion will assume the use of infinity-corrected microscope objectives. Slightly different considerations will apply when using a non-infinity corrected objectives (Bargmann and Avery, 1995).

The precision of laser surgery is best with the smallest possible focused spot. The beam waist diameter of a laser beam is inversely proportional to the range of angles converging onto the focus. This range of angles is maximized when the beam diameter is large enough to somewhat over-fill the back aperture of the objective. To determine whether the beam diameter is large enough, unscrew the objective and use a card to view the laser spot emerging from the objective mounting hole. Compare this size with the diameter of the lens at the back of the objective. Note that it is difficult to accurately estimate the diameter of a Gaussian beam by visual observation. Quantitative characterization of beam parameters can be performed by measuring the optical power transmitted through a centered aperture with variable diameter, or by using a beam analyzer (available from laser companies such as Coherent and Newport.)

The beam diameter can be increased by a Galilean telescope. This configuration of a Galilean telescope shown in Fig. 6 allows the beam diameter to be adjusted. If the separation between the lenses is decreased, the beam will diverge slightly as it leaves the telescope, so that its diameter will be larger at the objective. If the beam is larger than the objective, only the center will enter. Thus as the beam is expanded, less light enters the objective and the illumination becomes weaker. This can be a useful way of adjusting laser intensity and also improves the uniformity of the

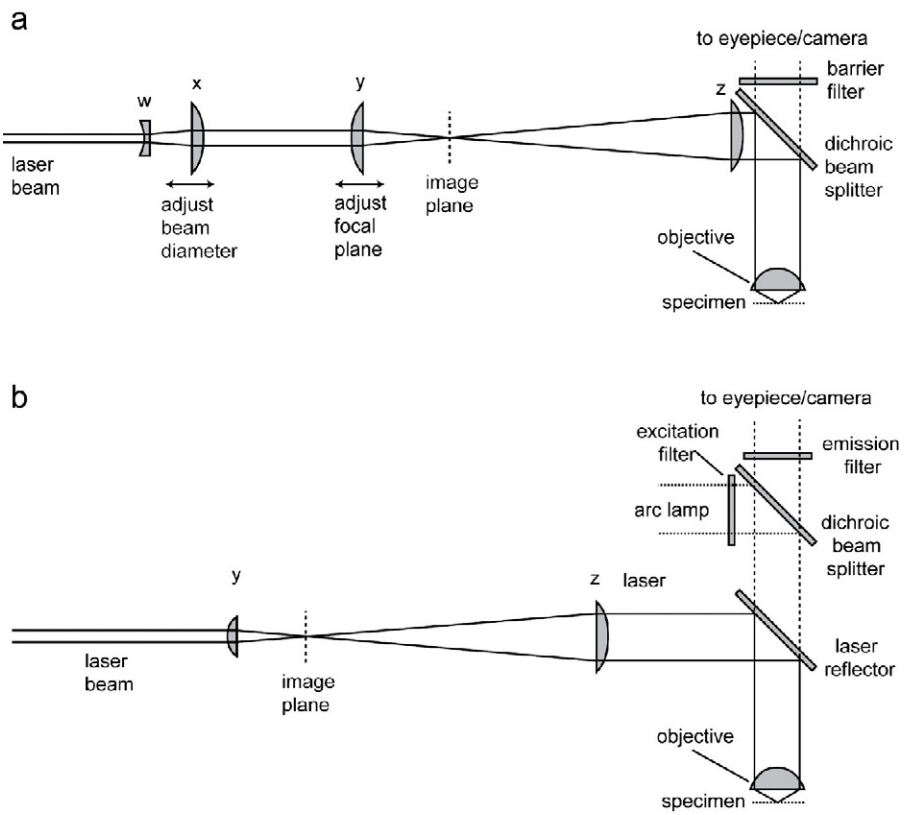

Fig. 6 Optics for laser ablation. (a) Beam coupling optics. Lenses *w* and *x* form a Galilean telescope. Beam diameter can be changed by moving lens x. The beam splitter reflects blue laser light into the specimen while passing longer wavelength light to the eyepiece so that the worm can be seen. The barrier filter prevents stray laser reflections from reaching the eyepiece. Lens *z* may be an additional lens you insert, or it may be part of the microscope. It may be more complex than a single lens. (b) A variation with filters arranged in a "stacked" configuration for simultaneous fluorescence microscopy and laser surgery.

illumination, as the center of the beam is the most uniform. Intensity can also be adjusted by interposing neutral density filters in the beam.

There is considerable flexibility in how the optical system is designed. For example, mirrors are often used to fold beam paths where space is constrained. Spatial filtering assemblies may be required if laser beam quality is poor.

The output of nanosecond lasers is usually triggered by manual control or foot pedal. The pulse frequency can be adjusted via a control panel. Femtosecond lasers normally generate pulses continuously, so that laser exposure to the sample must be controlled by an electromechanical or electro-optic shutter.

We now describe examples of nanosecond and femtosecond laser ablation systems similar to those used in our laboratories.

The optical configuration of our nanosecond ablation system corresponds approximately to Fig. 6a. It is a micropoint laser system, in which a small-dye laser-mounted directly on the microscope is pumped by a nitrogen laser coupled to it through a fiber optic cable. The dye solution is 5 mM coumarin 120 (7-amino-4-methylcoumarin) in ethanol. With this dye, the laser produces 3-nanosecond pulses of 440-nm light with an energy of about 30 mJ. The coupling optics include lenses to focus the beam to a point in an image of the specimen (lens *y* of Fig. 6a). The microscope is a Zeiss Axioskop with epifluorescence optics. In this case lens *z* of Fig. 6a corresponds to two lenses within the microscope that form the epifluorescence condenser. Laser light enters through the port on which an arc lamp would normally be mounted for excitation of fluorescence. On the Axioskop, this port is at the back.

The optical configuration of our femtosecond laser surgery system corresponds to Fig. 6b, except that the laser is coupled to an inverted microscope (Nikon TE2000). The laser is an acousto-optically cavity-dumped Ti:Sapphire laser (Kapteyn-Murnane Laboratories, Boulder, CO) producing 30–50 nJ pulses at 2 MHz repetition rate with 800 nm center wavelength. The repetition rate is reduced to 1 kHz via an electro-optic pulse picker (Eclipse, Kapteyn-Murnane Laboratories) triggered by a function generator. The beam enters a periscope, which modifies the beam height to match that of a second filter turret stacked above the first. The second filter turret contains a single filter cube, which contains a dichroic mirror selected to reflect the near-infrared laser radiation while passing shorter wavelengths. There is no emission or excitation filter in this filter cube. The first filter turret contains a normal set of fluorescence filter cubes for GFP, mCherry, etc. The laser is focused onto the sample through 60× or 100× Plan Apo oil-immersion objectives.

A detailed protocol for constructing a femtosecond laser surgery system can also be found in (Steinmeyer *et al*., 2010).

IV. Laser Killing of Cells

A. Procedures

1. Prepare Slide

Agar for slides consists of 2–5% agar in M9 or NGM buffer. Slide preparation is shown in Fig. 7. A drop of melted agar is placed on a slide and flattened into a pad. Two slides containing spacers (e.g., 1–3 layers of tape or coverslips) are used as guides for flattening the agar into a pad, so the final thickness of agar is equal to that of the spacer layer.

To immobilize animals for imaging and surgery, sodium azide (an inhibitor of mitochondrial respiration) at a concentration of 3–10 mM can be added to the melted agar. Animals subjected to azide anesthesia as L1 larvae have slightly slowed locomotion as adults, so mock ablation controls are advisable for any behavioral assay (J. Gray, unpublished observations). Azide arrests development, so it should be omitted

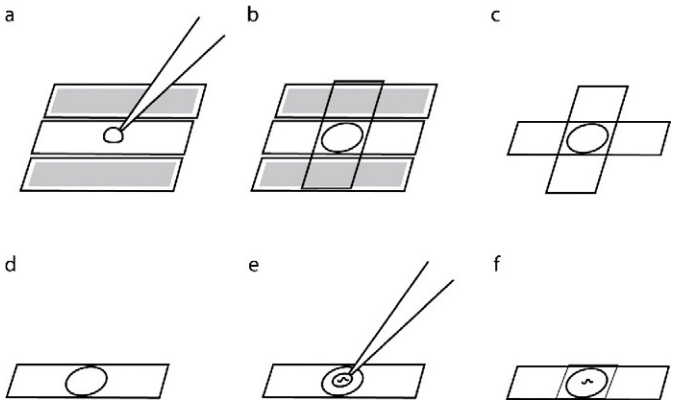

Fig. 7 Slide preparation. (a) Melted agar is placed on the surface of the slide. Spacers on slides shown in gray. (b) A second slide is used to flatten the agar into a thin pad. (c) Spacers are removed. To reduce drying of the pad, keep in this configuration until needed. (d) Remove top slide just before adding worms. (e) Add worm(s), liquid, and/or polystyrene beads, as needed. (f) Cover pad with coverslip.

if cell lineages will be followed. Azide is also usually omitted if embryonic cells will be killed. Other anesthetics that have been used to immobilize *C. elegans* include:

1. Levamisole, an acetylcholine agonist (Lewis *et al*., 1980) at a concentration of 1–10 mM. Tetramisole, the mixture of levamisole (the l-isomer) and dextramisole (the d-isomer), may also be used.
2. Muscimol, a GABA agonist (McIntire *et al*., 1993) at 1–10 mM.
3. 1-Phenoxy 2-propanol at 0.1–1% (Sulston and Horvitz, 1977).

An alternative to anesthetic immobilization is to add ~1 μL of a suspension of 0.05–0.1 μm diameter polystyrene microspheres (e.g., 08691–10 or 00876–15, 2.5% w/v suspension, Polysciences Corp., Warrington, PA) onto a 5% (or higher) agarose pad before picking worms onto the pad (C. F.-Yen, unpublished observations). The beads may increase the friction between the worm and the pad, opposing the worm's movement. The degree of immobilization depends on the concentration of agarose in the pad. In our experience, 10% agarose immobilizes the entire animal, while 5% agarose immobilizes the entire animal except for the tips of the nose and tail. The bead immobilization method allows for long-term imaging of unanesthetized, immobilized worms and rapid recovery of normal behavior after surgery, if needed. Immobilization is improved if the amount of bacteria transferred with the worms is minimized, and if the worms are arranged so that they do not come in contact with one another.

2. Place Worms on Slide at Dissecting Microscope

Place 1 μL of M9 on the agar. Pick up one or more worms with a platinum wire and elute them into the drop of M9 with gentle shaking. Count the worms in the

liquid, then place a coverslip on the slide. Avoid creating bubbles next to the worms, as air–water interfaces will interfere with imaging and laser surgery. As guide for finding the worms on the microscope, make a drawing of the worms on the slide and/or mark their positions on the back of the slide itself.

Prepare a set of control animals from the same plate. These animals should undergo mock ablations (identical time and conditions except for the laser surgery) and be rescued at the same time as the operated animals.

To facilitate cell identifications, slides should be prepared so that most animals are uniformly oriented on their left or right sides, as shown in Figs. 1–3. Animals will take this orientation if they are swimming actively when the coverslip is placed on the agar. For best results, (1) prepare slides quickly (2) treat animals gently, and (3) limit the amount of liquid on the slide to 1–2 μL.

If slide preparation is slow, many worms will be mounted so that their dorsal or ventral side is uppermost. If this orientation is desirable, use the higher recommended azide concentrations and place the coverslip on the slide after the worms have been anesthetized by the azide (this takes only a few minutes). Shift the coverslip very slightly after it is in place. Many of the worms should lodge in a ventral-up or dorsal-up position.

If cells are being killed in the embryo, mount embryos of the appropriate stage. If early embryos (<50 cells) are desired, they should be released from gravid hermaphrodites. Elute about 10 hermaphrodites into 10 μL of M9 on a microscope slide (without agar). As the animals swim in the liquid, cut them in half with a sharp razor blade by pressing them onto the glass slide. Eggs will be released into the liquid. Using a capillary pipette, move the eggs onto an agar pad without azide. To prevent air bubbles from forming, extra M9 can be placed on the slide before the coverslip is added. Cell lineages can be followed and cells killed as desired.

3. Use the Laser

For both nanosecond and femtosecond lasers, the coverslip assists in determining where the laser beam comes to a focus. For nanosecond pulses, fire the laser with focus on the coverslip. The laser will make a small permanent mark in the glass, visible under Nomarski microscopy. With femtosecond lasers, targeting into the coverslip produces a glowing spot of plasma at the focal point, visible only when the transmitted light illuminator is off. It is best imaged by a sensitive camera. Using the coverslip mark or plasma, the eyepiece, camera, and/or laser coupling optics should be adjusted so that the laser is optimally focused onto the imaging plane.

For initial alignment, adjust the coupling optics to bring the focal spot to approximately the center of the field of view. Move the micrometer in the eyepiece until it is aligned with the laser spot or mark the laser spot on the video/computer display if a camera is being used. Now the microscope stage and objective can be moved so that the laser focal point coincides with the target of interest.

Laser power can be varied by adjusting the controls on the laser, adding or removing neutral density filters between the laser and the scope, or by adjusting

the orientation of a polarizer through which the laser passes. Optimum power level is determined in part by target cell type. To kill neurons with a nanosecond laser, add filters until a nanosecond laser can just make a small hole in the coverslip. To kill larger cells such as hypodermal cells, reduce the neutral density filters so that the beam is about twice as intense. To kill large founder cells in the embryo, the beam should be about eight times as intense as needed to break holes in the coverslip. At these power levels, it should take between 20 and 200 laser pulses to kill a cell. If cell damage is observed more rapidly, the beam power should be reduced. While killing large nonneuronal cells requires more laser pulses, the procedure is easier because the larger size reduces the chance of collateral damage to other cells.

Animals can be located using the diagram prepared above (not necessary if the worms are all in one place). Animals may move during the recovery process, so it is best to target the same cell or group of cells in all of the animals on a single slide. During nanosecond laser killing of cells it is best to start by killing cells on the far side of the animal. Any nonspecific damage induced by firing the laser through the animal should be visible in the closer planes of focus. Animals in 3 mM azide can be kept on the slide for approximately 1 h, after which nonspecific cell damage and toxicity are observed. At 10 mM azide, animals should be kept on the slide no longer than 15 min.

4. Monitor Damage

After laser killing, any one of the following kinds of damage may be considered sufficient to kill the cell:

Nucleus disappears
Nucleus takes on a button-like appearance characteristic of programmed cell death (Sulston and Horvitz, 1977).
Nucleus changes in refractive index and cell boundary becomes clearly visible (Fig. 8).
Scar from laser transects nucleus (Fig. 8).

If the targeted cell expresses GFP, fluorescence imaging can be useful for aiming the laser and monitoring cell killing. Substantial photobleaching/disruption of the fluorescent marker is usually observed. However, loss of GFP fluorescence does not imply that a cell has been killed, as the GFP may be merely photobleached. Imaging the cell by Nomarski optics is critical for verifying damage.

Damage may take up to 30 min to develop but is usually visible within 1 min of the operation. Discard the animal if a basement membrane is punctured (recognized as the sudden appearance of a fluid-filled pocket that expands near the site of ablation, Fig. 8c or massive leakage of GFP into the intercellular space). Discard any animals in which the cuticle is punctured (visible as oozing or bubbling of material from the animal near the site of the operation).

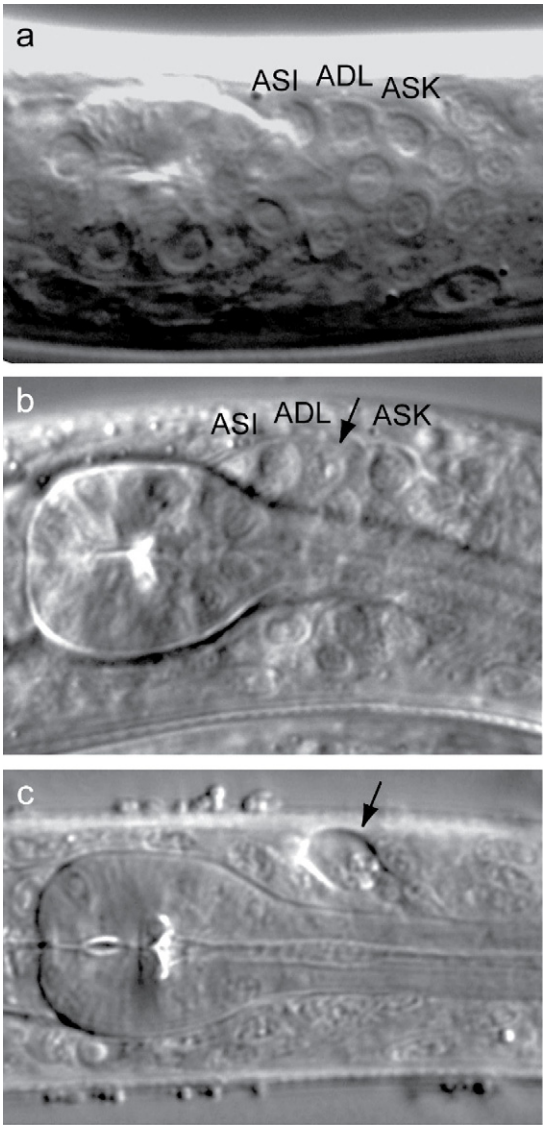

Fig. 8 Laser damage. (a) Nomarski image showing ASI, ADL, ASK nuclei. (b) Similar image after laser ablation of ADL nucleus. Note bright refractile scar in nucleus and loss of contrast at nuclear boundary. (c) A ruptured basement membrane. Arrow points to fluid-filled cavity.

Kill all undesired animals on the slide by puncturing the cuticle with the laser, which will cause the worm to burst. Puncture of the cuticle is easiest in the posterior of the animal. Laser power can also be increased to kill worms. If all extra animals are killed, the rescue step is easier because only desired animals are viable.

5. Rescue Animals

Draw 1–2 μL of M9 into a drawn-out capillary pipette. If anesthetics are used for immobilization, slide the coverslip off the slide very gently without pressing down on the coverslip. If this is done smoothly, the worms will remain in place and can be located using the diagrams prepared at the beginning. If polystyrene beads are used for immobilization, pull the coverslip directly upward without sliding to avoid damaging animals.

After laser surgery, the worms may be fragile. Using suction, release a bit of liquid from the capillary pipette, draw the worm into the pipette, and release the worm onto a seeded NGM plate. With azide immobilization, the worm should start moving again within 15 min. With bead immobilization, the worm should recover almost immediately. Confirm the specificity of the operation as described below.

B. Experimental Design and Controls

Interpreting the result of laser killing depends on the answers to two questions: (1) Has the operated cell lost all function? (2) Have additional cell types been damaged? Because the nucleus is the structure most easily visualized by Nomarksi optics, laser damage is usually assessed by the appearance of the nucleus; however, cells may function even in the absence of a nucleus. For example, when the nuclei of the touch cells are killed in the third larval stage, touch cell processes and function are maintained in the adult (Chalfie *et al*., 1985).

Killing nuclei early in development maximizes the chances that they will lose function, but can increase the likelihood of compensatory changes. In males, adult ablation of certain sensory neurons reduces attraction to hermaphrodites, but ablation of the same neurons before sexual maturation does not, presumably because of compensation among neurons (White *et al*., 2007).

In general, killing a cell nucleus in the first larval stage appears to eliminate cell function by the adult stage. For several types of neuronal cells, functional data and electron microscopy confirm that neuronal processes lose function within 24–48 h if the nucleus is damaged by the laser in the first larval stage (Avery and Horvitz, 1987, 1989; Bargmann and Horvitz, 1991a).

What is the fate of the remnants of the killed cell? While it is possible that corpses of laser-killed cells are sometimes engulfed by neighboring cells in a similar manner to that of programmed cell death, such clearance does not always occur. Refractile remains of a destroyed nucleus can often be seen in DIC days after the laser surgery. Electron microscopy reconstructions of pharynxes in which most of the neurons had been killed also showed many nuclear remnants and a few process remnants, which were extremely attenuated (Avery and Horvitz, 1989). Similarly, electron microscopy reconstructions after L1 ablation of amphid neurons showed electron-dense remnants of the cilia with diameter much smaller than that of the normal cilia (C. I. Bargmann, unpublished observations).

An alternative to directly killing the cell of interest is to kill its precursor during development so that the cell is never generated. This approach often leads to the elimination of several cell types. It is especially important to examine adjacent cells for any changes in cell fate when precursor cells are killed. Most cell interactions are confined to a short period (minutes to hours), so the timing of cell killing is particularly important when cell interactions take place. In addition to technical issues, other issues might confound the interpretation of cell killing results:

1. Redundancy

In several cases, a particular defect is observed only when several cell types are all killed together (Avery and Horvitz, 1989; Bargmann and Horvitz, 1991b; McIntire *et al*., 1993). Therefore, killing one cell may reveal only a subset of the functions of that cell.

2. Multiple Functions of One Cell

If a cell participates in distinct biological processes, some effects may be hard to observe. For example, if a cell is essential for viability, it will not be possible to determine whether it functions in a behavior. Also, the death of one cell may have indirect effects on the development, survival, or functions of other cell types.

V. Assessing Damage to the Operated Cell

After laser operation, it is important to verify that the targeted cell has been removed. The amount and timing of damage required to eliminate a given cell are determined empirically, using the following guidelines:

1. Closely observe the cell of interest and adjacent cells during, and for 5–10 min following, laser exposure.
2. Confirm cell death at least 1 h after the operation (remount the animal on a slide, search for the killed cell, and examine cells in the vicinity). It is often convenient to perform this step at the end of an experiment.
3. If possible, confirm cell identity and cell death by some method other than observing the nucleus and/or cell fluorescence. For example, if an antibody is known to recognize the cell of interest or nearby cells, animals can be stained with the antiserum after laser killing of the cell. Other functions of the cell may also be assessed. These experiments often require that the animal be killed and may be practical only after the end of the experiment.
4. If possible, compare the results of killing a cell and killing precursors to that cell.

VI. Unintended Damage

The simplest way to establish that cells adjacent to the killed cell are intact, is to observe their appearance, and function directly. After killing a cell, antibodies or assays specific for adjacent cells can be used to determine whether those cells are normal. If an effect of killing a cell is seen, it is also useful to kill all of the surrounding cells and not the cell of interest. This control can ensure that removing the targeted cell causes a particular effect.

The death of a cell might retard development or stunt growth. Be aware, however, that accidental damage to the pharynx or cuticle will also retard development. To verify that a specific cell death retards development, cell killing protocols can be modified to minimize nonspecific effects of the operation. Reducing the amount of time the animals spend under anesthesia to less than 15 min leads to faster and more efficient recovery. Short times under azide should be used for any protocol in which development is slowed. Reducing the power of the laser beam by using neutral density filters decreases unintended laser damage, so minimal laser energy should be used in all experiments.

VII. Laser Cutting of Nerve Fibers

A. Experimental Procedures

Procedures for laser-cutting of nerve fibers are similar to whole-cell ablations with one major difference: because nerve processes are not visible with DIC, the structures to be cut must be labeled with fluorescent reporter, and cell process identification and laser procedures must be performed via fluorescence imaging. Nomarski microscopy can still be used for aligning worms for surgery and assessing damage in operated worms.

Preparation of pads and worms for laser cutting is identical to those for whole-cell ablation. If nerve cutting is being done to image the resulting regrowth (Fig. 10), an anesthetic-free immobilization method using polystyrene microspheres might be preferable.

After finding worms under bright-field or Nomarski optics, switch to fluorescence imaging and observe the process or processes to be cut. The location of the cut may be measured relative to the cell body or another anatomical landmark. Adjust the stage and object focus to align the intended cut point at the laser spot position, previously marked as described above. Fire the laser by triggering an electronic shutter or laser modulator for a specified time. Laser damage should result in a distinct gap in the fluorescence of the nerve fiber (Figs. 9 and 10).

Note that damage to nearby unlabeled cells or the cuticle may not be visible under fluorescence microscopy. Monitoring of possible damage in neighboring tissues using Nomarski microscopy is recommended, especially while establishing laser exposure protocols.

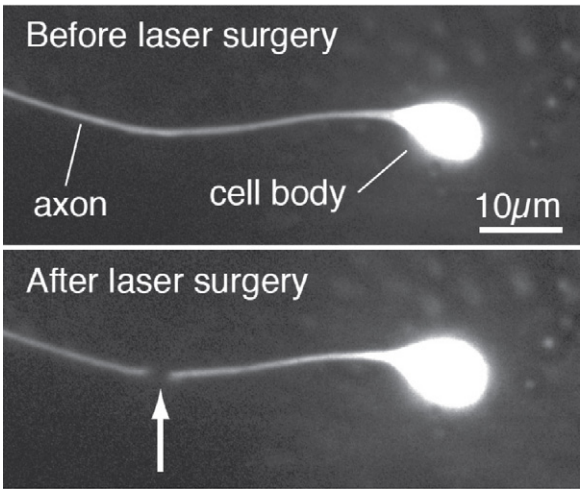

Fig. 9 Femtosecond laser axotomy of a GFP-labeled ALM neuron. Arrow shows location of cut. Reprinted from Gabel (2008).

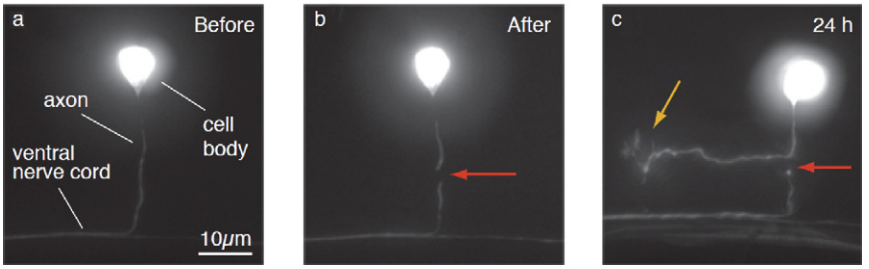

Fig. 10 Nerve regeneration after laser axotomy. (a) GFP-labeled AVM cell body and axon projecting into ventral nerve cord. (b) Immediately after laser surgery. Arrow shows location of cut. (c) 24 h after laser surgery. Arrows show location of cut (at right) and axotomy-induced growth cone (at left). Reprinted from Gabel (2008). (For color version of this figure, the reader is referred to the web version of this book.)

Since nerve fibers are very thin, cutting them requires a higher degree of precision during the laser surgery procedure, compared to whole-cell ablation. We find that laser targeting is easier with a motorized, high-resolution microscope stage than with a manually controlled stage.

B. Experimental Design and Interpretation

An important difference between cell killing and laser axotomy concerns unintended damage. Since nerve fibers are generally smaller in diameter than the laser

damage spot size (~0.5–1 μm), some degree of damage to surrounding tissues is usually unavoidable (by contrast, during cell killing almost all laser damage should occur within the nucleus.) Where two or more processes run together in a bundle, severing one fiber may also damage other fibers in the bundle. As a result, most laser surgery of nerve processes has been limited to the relatively few processes which extend independently (or almost independently), thus providing a "clear shot" of an individual process. Examples include the gentle touch mechanosensory cells, the motor neuron commissures, and the processes of the HSN neuron (Ghosh-Roy and Chisholm, 2010). Individual sensory dendrites separated from neighbors by a few microns have been severed using a femtosecond laser (Chung *et al*., 2006).

When designing experimental procedures and controls, consideration should be given to what neighboring tissues will be damaged. Where results of laser surgeries in two groups are to be compared, particular care should be taken to ensure that identical laser parameters are used. For example, it has been shown that the rate of regeneration after axotomy depends on the pulse energies used (Bourgeois and Ben-Yakar, 2007), possibly due to different amounts of damage to tissues surrounding the axon.

Another form of unintended damage in nerve cutting is that amputation of the axon can cause damage to the cell body. This unintended effect can complicate the interpretation of experiments, particularly those that hinge on measuring behavioral or physiological differences between the effects of cell killing and nerve fiber cutting. Imaging the cell body by fluorescence and/or Nomarski at the time of assays may give some indication about the extent of injury. Demonstration of normal calcium signals in the cell body may also be informative (Zhang *et al*., 2008).

Insufficient laser power might not cut the axon but instead induce photobleaching of GFP in the exposed segment. This results in a gap in fluorescence with the appearance of an axotomy. How can you tell whether a nerve process has been cut rather than merely photobleached? First, retraction of the severed ends immediately after laser exposure, indicating a release of tension in the nerve fiber, can indicate that the nerve has been cut. Second, photobleached processes will gradually recover within a few minutes as unbleached GFP diffuses back into the illuminated region, whereas truly severed ends will remain stable.

VIII. Related Methods

Laser surgery can be a precise and versatile tool for eliminating or damaging specific cells in an animal. Its utility is often limited, however, by the difficulty of identifying each cell, particularly during development, and by the relatively slow ablation process. Several current and emerging techniques are useful for killing defined cells in larger numbers of animals.

A. Genetic Ablation

Cells can be killed by using cell-specific promoters to express cytotoxic products. Such genetic ablation can be much more efficient than laser ablation since it eliminates the need for manual cell killing. Strains containing cell-killing transgenes can be maintained easily and used for genetic screens.

Several methods for genetic ablation have been developed. Dominant alleles of *mec-4* and a related genes of the degenerin/ENaC family lead to the deaths of the 6 mechanosensory cells (Chalfie and Wolinsky, 1990; Driscoll and Chalfie, 1991). Ectopic expression of these alleles, collectively denoted as *mec-4(d)*, can be used to disrupt function in a wide range of cells (Harbinder *et al*., 1997). *mec-4(d)* Transgenes vary considerably in their toxicity to different cell types, however, in part based on the cooperating gene *mec-6*.

A similar strategy has been developed using the cell-death genes *ced-3*, *ced-4*, and *egl-1* (Conradt and Horvitz, 1998; Shaham and Horvitz, 1996). For example, EGL-1 expressed under a cell-specific promoter was used to kill the pharyngeal neuron M3 (Rauthan *et al*., 2007). Similarly, a human caspase was used to kill subsets of locomotory command interneurons (Zheng *et al*., 1999).

One limitation of these genetic ablation methods is that cell-specific promoters are often not available for a given cell, or are associated with "leakiness" which may affect nontargeted cells. To overcome these limitations, a two-component system based on reconstituted caspases has been developed (Chelur and Chalfie, 2007). Separate expression of two subunits of *C. elegans* CED-3 or human caspase-3 from a combination of promoters resulted in reconstituted caspase activity, and therefore cell death, only in cells in which both promoters are active. The authors also demonstrated inducible cell killing by expressing one subunit under a heat-shock promoter.

A different type of genetic manipulation has been used to sever nerve fibers. In mutants for beta spectrin (*unc-70*), motor axons are fragile and spontaneously break during normal movement of the worm (Hammarlund *et al*., 2007). An RNAi screen for axon regeneration phenotypes in an *unc-70* background revealed that axonal regeneration requires the MAP kinase pathway (Hammarlund *et al*., 2009); this requirement was subsequently confirmed by laser axotomy experiments.

B. Photoablation

Photosensitizers are agents that generate toxic reactive oxygen species upon optical irradiation, and can be used to inactivate selected proteins or for light-induced cell killing. Green light illumination of cells expressing KillerRed, a fluorescent protein engineered for high phototoxicity (Bulina *et al*., 2006) has been used to kill *C. elegans* neurons (Marc Hammarlund and Daniel Williams, personal communication). Green light illumination can be delivered by placing a number of worms in a droplet under a fluorescence stereo microscope. The KillerRed system possesses some advantages of both genetic and laser ablation. It can be used to ablate

genetically defined cells in large numbers of worms, but also allows the timing of cell killing to be controlled. It is also possible to achieve some degree of spatial selectivity by illuminating a restricted subset of cells, albeit on an individual basis.

C. Microfluidics

Microfluidics refers to a set of technologies for manipulation of fluids in microliter and sub-microliter volumes using devices fabricated by "soft lithography" techniques (Whitesides, 2006). A number of microfluidic devices have been developed for use with *C. elegans,* and have the potential to increase the throughput of many procedures, including laser surgeries.

Hulme *et al*. developed a device for trapping of up to 128 worms in tapered microfluidic channels (Hulme *et al*., 2007). One of us (C. V. Gabel) has used these clamps to perform laser axotomy and long-term imaging of axonal regrowth in multiple animals simultaneously. Several groups have developed microfluidic devices for serially immobilizing, imaging, manipulating, and sorting worms. By combining microfluidic technology with laser surgery methods, semi-automated systems for laser axotomy (Guo *et al*., 2008; Rohde *et al*., 2007; Zeng *et al*., 2008) and whole-cell ablation (Chung and Lu, 2009; Chung *et al*., 2008) have been demonstrated. The usefulness and impact of these devices will grow as they become more widely available to the *C. elegans* research community.

Acknowledgments

We thank John Sulston and Ron Ellis for allowing us to include Figs. 2 and 4 and Fig. 3, respectively, and Niels Ringstad for helpful comments. This work was supported by the National Science Foundation and National Institutes of Health.

References

Austin, J., and Kimble, J. (1987). *glp-1* is required in the germ line for regulation of the decision between mitosis and meiosis in *C. elegans*. *Cell* **51**, 589–599.

Avery, L., and Horvitz, H. R. (1987). A cell that dies during wild-type *C. elegans* development can function as a neuron in a *ced-3* mutant. *Cell* **51**, 1071–1078.

Avery, L., and Horvitz, R. (1989). Pharyngeal pumping continues after laser killing of the pharyngeal nervous-system of *C. elegans*. *Neuron* **3**, 473–485.

Bargmann, C. I., and Avery, L. (1995). Laser killing of cells in *Caenorhabditis elegans*. *In* "*C elegans*: Modern Biological Analysis of an Organism," (H. Epstein, and D. Shakes, eds.), pp. 225–250. Academic Press, New York.

Bargmann, C. I., Hartwieg, E., and Horvitz, H. R. (1993). Odorant-selective genes and neurons mediate olfaction in *C. elegans*. *Cell* **74**, 515–527.

Bargmann, C. I., and Horvitz, H. R. (1991a). Chemosensory neurons with overlapping functions direct chemotaxis to multiple chemicals in *C. elegans*. *Neuron* **7**, 729–742.

Bargmann, C. I., and Horvitz, H. R. (1991b). Control of larval development by chemosensory neurons in *Caenorhabditis elegans*. *Science* **251**, 1243–1246.

Bourgeois, F., and Ben-Yakar, A. (2007). Femtosecond laser nanoaxotomy properties and their effect on axonal recovery in *C. elegans*. *Optics Exp.* **15**, 8521–8531.

Bulina, M. E., Chudakov, D. M., Britanova, O. V., Yanushevich, Y. G., Staroverov, D. B., Chepurnykh, T. V., Merzlyak, E. M., Shkrob, M. A., Lukyanov, S., and Lukyanov, K. A. (2006). A genetically encoded photosensitizer. *Nat. Biotechnol.* **24**, 95–99.

Burket, C. T., Higgins, C. E., Hull, L. C., Berninsone, P. M., and Ryder, E. F. (2006). The *C. elegans* gene dig-1 encodes a giantmember of the immunoglobulin superfamily that promotes fasciculationof neuronal processes. *Dev. Biol.* **299**, 193–205.

Chalfie, M., Sulston, J. E., White, J. G., Southgate, E., Thomson, J. N., and Brenner, S. (1985). The neural circuit for touch sensitivity in *Caenorhabditis elegans*. *J. Neurosci.* **5**, 956–964.

Chalfie, M., and Wolinsky, E. (1990). The identification and suppression of inherited neurodegeneration in *Caenorhabditis elegans*. *Nature* **345**, 410–416.

Chamberlin, H. M., and Sternberg, P. W. (1993). Multiple cell interactions are required for fate specification during male spicule development in *Caenorhabditis elegans*. *Development* **118**, 297–324.

Chelur, D. S., and Chalfie, M. (2007). Targeted cell killing by reconstituted caspases. *Proc. Natl. Acad. Sci. USA* **104**, 2283–2288.

Chiang, J. T. A., Steciuk, M., Shtonda, B., and Avery, L. (2006). Evolution of pharyngeal behaviors and neuronal functions in free-living soil nematodes. *J. Exp. Biol.* **209**, 1859–1873.

Chung, K., and Lu, H. (2009). Automated high-throughput cell microsurgery on-chip. *Lab Chip* **9**, 2764–2766.

Chung, K. H., Crane, M. M., and Lu, H. (2008). Automated on-chip rapid microscopy, phenotyping and sorting of *C. elegans*. *Nat. Methods* **5**, 637–643.

Chung, S. H., Clark, D. A., Gabel, C. V., Mazur, E., and Samuel, A. D. T. (2006). The role of the AFD neuron in *C. elegans* thermotaxis analyzed using femtosecond laser ablation. *BMC Neurosci.* **7**, 30.

Clark, D. A., Biron, D., Sengupta, P., and Samuel, A. D. T. (2006). The AFD sensory neurons encode multiple functions underlying thermotactic behavior in *Caenorhabditis elegans*. *J. Neurosci.* **26**, 7444–7451.

Collet, J., Spike, C. A., Lundquist, E. A., Shaw, J. E., and Herman, R. K. (1998). Analysis of osm-6, a gene that affects sensory cilium structure and sensory neuron function in *Caenorhabditis elegans*. *Genetics* **148**, 187–200.

Conradt, B., and Horvitz, H. R. (1998). The *C. elegans* protein EGL-1 is required for programmed cell death and interacts with the Bcl-2-like protein CED-9. *Cell* **93**, 519–529.

Desai, C., and Horvitz, H. R. (1989). *Caenorhabditis elegans* mutants defective in the functioning of the motor neurons responsible for egg-laying. *Genetics* **121**, 703–721.

Driscoll, M., and Chalfie, M. (1991). The *mec-4* gene is a member of a family of *Caenorhabditis elegans* genes that can mutate to induce neuronal degeneration. *Nature* **349**, 588–593.

Ferguson, E. L., and Horvitz, H. R. (1985). Identification and characterization of 22 genes that affect the vulval cell lineages of the nematode *Caenorhabditis elegans*. *Genetics* **110**, 17–72.

Forbes, W. M., Ashrton, F. T., Boston, R., Zhu, X., and Schard, G. A. (2004). Chemoattraction and chemorepulsion of *Strongyloides stercoralis* infective larvae on a sodium chlroide gradient is mediated by amphidical neuron pairs ASE and ASH, respectively. *Vet. Parasitol.* **123**, 215–221.

Gabel, C. V. (2008). Femtosecond lasers in biology: nanoscale surgery with ultrafast optics. *Contemp. Phys.* **49**, 391–411.

Gabel, C. V., Antoine, F., Chuang, C. F., Samuel, A. D. T., and Chang, C. (2008). Distinct cellular and molecular mechanisms mediate initial axon development and adult-stage axon regeneration in *C. elegans*. *Development* **135**, 3623.

Gabel, C. V., Gabel, H., Pavlichin, D., Kao, A., Clark, D. A., and Samuel, A. D. T. (2007). Neural circuits mediate electrosensory behavior in *Caenorhabditis elegans*. *J. Neurosci.* **27**, 7586–7596.

Garriga, G., Desai, C., and Horvitz, H. R. (1993). Cell interactions control the direction of outgrowth, branching and fasciculation of the HSN axons of *Caenorhabditis elegans*. *Development* **117**, 1071–1087.

Ghosh-Roy, A., and Chisholm, A. D. (2010). *Caenorhabditis elegans*: A new model organism for studies of axon regeneration. *Dev. Dynamics* **239**, 1460–1464.

Ghosh-Roy, A., Wu, Z., Goncharov, A., Jin, Y., and Chisholm, A. D. (2010). Calcium and cyclic AMP promote axonal regeneration in *Caenorhabditis elegans* and require DLK-1 kinase. *J. Neurosci.* **30**, 3175–3183.

Gray, J. M., Hill, J. J., and Bargmann, C. I. (2005). A circuit for navigation in *Caenorhabditis elegans*. *Proc. Natl. Acad. Sci. USA* **102**, 3184–3191.

Guo, S. X., Bourgeois, F., Chokshi, T., Durr, N. J., Hilliard, M. A., Chronis, N., and Ben-Yakar, A. (2008). Femtosecond laser nanoaxotomy lab-on-achip for *in vivo* nerve regeneration studies. *Nat. Methods* **5**, 531–533.

Hammarlund, M., Jorgensen, E. M., and Bastiani, M. J. (2007). Axons break in animals lacking beta-spectrin. *J. Cell Biol.* **176**, 269–275.

Hammarlund, M., Nix, P., Hauth, L., Jorgensen, E. M., and Bastiani, M. (2009). Axon regeneration requires a conserved MAP kinase pathway. *Science* **323**, 802–806.

Harbinder, S., Tavernarakis, N., Herndon, L. A., Kinnell, M., Xu, S. Q., Fire, A., and Driscoll, M. (1997). Genetically targeted cell disruption in *Caenorhabditis elegans*. *Proc. Natl. Acad. Sci. USA* **94**, 13128–13133.

Hedgecock, E. M., Culotti, J. G., Thomson, J. N., and Perkins, L. A. (1985). Axonal guidance mutants of *Caenorhabditis elegans* identified by filling sensory neurons with fluorescein dyes. *Dev. Biol.* **111**, 158–170.

Hulme, S. E., Shevkoplyas, S. S., Apfeld, J., Fontana, W., and Whitesides, G. M. (2007). A microfabricated array of clamps for immobilizing and imaging *C. elegans*. *Lab Chip* **7**, 1515–1523.

Kimble, J. (1981). Alterations in cell lineage following laser ablation of cells in the somatic gonad of *Caenorhabditis elegans*. *Dev. Biol.* **87**, 286–300.

Kimble, J., and Hirsh, D. (1979). Post-embryonic cell lineages of the hermaphrodite and male gonads in *Caenorhabditis elegans*. *Dev. Biol.* **70**, 396–417.

Kimble, J. E., and White, J. G. (1981). On the control of germ-cell development in *Caenorhabditis elegans*. *Dev. Biol.* **81**, 208–219.

Lewis, J. A., Wu, C. -H., Berg, H., and Levine, J. H. (1980). The genetics of levamisole resistance in the nematode *Caenorhabditis elegans*. *Genetics* **95**, 905–928.

Li, C., and Chalfie, M. (1990). Organogenesis in *C. elegans* – positioning of neurons and muscles in the egg-laying system. *Neuron* **4**, 681–695.

Li, W., Feng, Z. Y., Sternberg, P. W., and Xu, X. Z. S. (2006). A *C. elegans* stretch receptor neuron revealed by a mechanosensitive TRP channel homologue. *Nature* **440**, 684–687.

McIntire, S. L., Jorgensen, E., Kaplan, J., and Horvitz, H. R. (1993). The GABAergic nervous system of *Caenorhabditis elegans*. *Nature* **364**, 337–341.

Mello, C. C., Draper, B. W., Krause, M., Weintraub, H., and Priess, J. R. (1992). The Pie-1 and Mex-1 genes and maternal control of blastomere identity in early *C. elegans* embryos. *Cell* **70**, 163–176.

Priess, J. R., and Thomson, J. N. (1987). Cellular interactions in early *C. elegans* embryos. *Cell* **48**, 241–250.

Rauthan, M., Morck, C., and Pilon, M. (2007). The *C. elegans* M3 neuron guides the growth cone of its sister cell M2 via the Kruppel-like zinc finger protein MNM-2. *Dev. Biol.* **311**, 185–199.

Rohde, C. B., Zeng, F., Gonzalez-Rubio, R., Angel, M., and Yanik, M. F. (2007). Microfluidic system for on-chip high-throughput whole-animal sorting and screening at subcellular resolution. *Proc. Natl. Acad. Sci. USA* **104**, 13891–13895.

Schnabel, R. (1994). Autonomy and nonautonomy in cell fate specification of muscle in the *Caenorhabditis elegans* embryo – a reciprocal induction. *Science* **263**, 1449–1452.

Shaham, S., and Horvitz, H. R. (1996). Developing *Caenorhabditis elegans* neurons may contain both cell-death protective and killer activities. *Genes Dev* **10**, 578–591.

Shen, N., Datta, D., Schaffer, C. B., LeDuc, P., Ingber, D. E., and Mazur, E. (2005). Ablation of cytoskeletal filaments and mitochondria in live cells using a femtosecond laser nanoscissor. *Mech. Chem. Biosyst.* **2**, 17–25.

Sommer, R. J., and Sternberg, P. W. (1994). Changes of induction and competence during the evolution of vulva development in nematodes. *Science* **265**, 114–118.

Srinivasan, J., Durak, O., and Sternberg, P. W. (2008). Evolution of a polymodal sensory response network. *BMC Biol.* **6**, 52.

Steinmeyer, J. D., Gilleland, C. L., Pardo-Martin, C., Angel, M., Rohde, C. B., Scott, M. A., and Yanik, M. F. (2010). Construction of a femtosecond laser microsurgery system. *Nat. Prot.* **5**, 395–407.

Sulston, J. E., and Horvitz, H. R. (1977). Post-embryonic cell lineages of nematode, *Caenorhabditis elegans*. *Dev. Biol.* **56**, 110–156.

Sulston, J. E., Schierenberg, E., White, J. G., and Thomson, J. N. (1983). The embryonic-cell lineage of the nematode *Caenorhabditis elegans*. *Dev. Biol.* **100**, 64–119.

Sulston, J. E., and White, J. G. (1980). Regulation and cell autonomy during post-embryonic development of *Caenorhabditis elegans*. *Dev. Biol.* **78**, 577–597.

Thomas, J. H., Stern, M. J., and Horvitz, H. R. (1990). Cell-interactions coordinate the development of the *C. elegans* egg-laying system. *Cell* **62**, 1041–1052.

Trent, C., Wood, W. B., and Horvitz, H. R. (1988). A novel dominant transformer allele of the sex-determining gene Her-1 of *Caenorhabditis elegans*. *Genetics* **120**, 145–157.

Tsalik, E. L., and Hobert, O. (2003). Functional mapping of neurons that control locomotory behavior in *Caenorhabditis elegans*. *J. Neurobiol.* **56**, 178–197.

Vogel, A., Noack, J., Huttman, G., and Paltauf, G. (2005). Mechanisms of femtosecond laser nanosurgery of cells and tissues. *Appl. Phys. B – Lasers Opt.* **81**, 1015–1047.

Vogel, A., and Venugopalan, V. (2003). Mechanisms of pulsed laser ablation of biological tissues. *Chem. Rev.* **103**, 577–644.

Walthall, W. W., and Chalfie, M. (1988). Cell–cell interactions in the guidance of late-developing neurons in *Caenorhabditis elegans*. *Science* **239**, 643–645.

Ward, A., Liu, J., Feng, Z. Y., and Xu, X. Z. S. (2008). Light-sensitive neurons and channels mediate phototaxis in *C. elegans*. *Nat. Neurosci.* **11**, 916–922.

Waring, D. A., and Kenyon, C. (1990). Selective silencing of cell communication influences anteroposterior pattern-formation in *C. elegans*. *Cell* **60**, 123–131.

White, J. Q., Nicholas, T. J., Gritton, J., Truong, L., Davidson, E. R., and Jorgensen, E. M. (2007). The sensory circuitry for sexual attraction in *C. elegans* males. *Curr. Biol.* **17**, 1847–1857.

Whitesides, G. M. (2006). The origins and the future of microfluidics. *Nature* **442**, 368–373.

Wu, Z., Ghosh-Roy, A., Yanik, M. F., Zhang, A. Z., Jin, Y. S., and Chisholm, A. D. (2007). *Caenorhabditis elegans* neuronal regeneration is influenced by life stage, ephrin signaling, and synaptic branching. *Proc. Natl. Acad. Sci. USA* **104**, 15132–15137.

Yan, D., Wu, Z. L., Chisholm, A. D., and Jin, Y. S. (2009). The DLK-1 kinase promotes mRNA stability and local translation in *C. elegans* synapses and axon regeneration. *Cell* **138**, 1005–1018.

Yanik, M. F., Cinar, H., Cinar, H. N., Chisholm, A. D., Jin, Y. S., and Ben-Yakar, A. (2004). Neurosurgery – functional regeneration after laser axotomy. *Nature* **432**, 822.

Zeng, F., Rohde, C. B., and Yanik, M. F. (2008). Sub-cellular precision on-chip small-animal immobilization, multi-photon imaging and femtosecond-laser manipulation. *Lab Chip* **8**, 653–656.

Zhang, M., Chung, S. H., Fang-Yen, C., Craig, C., Kerr, R. A., Suzuki, H., Samuel, A. D. T., Mazur, E., and Schafer, W. R. (2008). A self-regulating feed-forward circuit controlling *C. elegans* egg-laying behavior. *Curr. Biol.* **18**, 1445–1455.

Zheng, Y., Brockie, P. J., Mellem, J. E., Madsen, D. M., and Maricq, A. V. (1999). Neuronal control of locomotion in *C. elegans* is modified by a dominant mutation in the GLR-1 ionotropic glutamate receptor. *Neuron* **24**, 347–361.